

---

# Ancient TL

www.ancienttl.org · ISSN: 2693-0935

---

Tribolo, C., Kreutzer, S. and Mercier, N., 2019. *How reliable are our beta-source calibrations?*  
Ancient TL 37(1): 1-10. <https://doi.org/10.26034/la.atl.2019.529>

This article is published under a *Creative Commons Attribution 4.0 International* (CC BY):  
<https://creativecommons.org/licenses/by/4.0>



© The Author(s), 2019

## How reliable are our beta-source calibrations?

Chantal Tribolo<sup>1\*</sup>, Sebastian Kreutzer<sup>1</sup>, Norbert Mercier<sup>1</sup>

<sup>1</sup> IRAMAT-CRP2A, UMR 5060, CNRS – Université Bordeaux Montaigne, 33607, Pessac Cedex, France

\*Corresponding Author: ctribolo@u-bordeaux-montaigne.fr

*Received: November 29, 2018; in final form: April 18, 2019*

### Abstract

The calibration of any artificial  $\beta$ -source attached to a luminescence reader is fundamental for the accuracy of luminescence dating results. Here, we present calibration results obtained for a  $\beta$ -source attached to a single grain Risø reader in Bordeaux using a series of quartz of different origins. The quartz was irradiated with three different  $\gamma$ -irradiators. An unexpected variability of the apparent dose rates was observed and our results suggest that the  $\gamma$ -irradiation is the main reason for this variability. Further work is needed to clarify the underlying reasons.

**Keywords:** Source calibration; luminescence dating; quartz

Göksu et al. 1995; Kadereit & Kreutzer 2013; Guérin & Valadas 2014).

In practice, natural materials (e.g., quartz, flint, quartzite pebbles, feldspars, calcite, ...) similar to those dated with the luminescence methods are usually preferred for calibration (e.g., Pernicka & Wagner, 1979), although alternatives based on artificial materials (e.g.,  $\text{Al}_2\text{O}_3\text{:C}$ ,  $\text{CaF}_2$ ) have also been suggested in the past (e.g., Erfurt et al., 2001). Nowadays, quartz appears to be the most commonly dated natural mineral with luminescence methods. Hence, using quartz for  $\beta$ -source calibration appears to be a logical step, providing its luminescence properties are suitable for high-precision calibration work. To date, two types of ‘calibration quartz’ are commercially available: from the Risø National Laboratory (DTU Nutech) (Hansen et al., 2015, 2018), henceforth named ‘Risø calibration quartz’ (RCQ), and more recently from Freiberg Instruments GmbH (D. Richter, pers. comm.), henceforth named LexCal2014 quartz (LCQ). In both cases, batch numbers (#) are assigned to distinguish between calibration materials prepared and irradiated at different times.

The RCQ and the LCQ, in conjunction with the single aliquot regenerative (SAR) dose protocol (Murray & Wintle, 2000) provide a convenient way of obtaining dose rate values for many laboratories worldwide. However, and despite of the tests that have been carefully run on these materials before they were shipped to the luminescence community (Hansen et al. 2015; Hansen et al. 2018; D. Richter, pers. comm.), this ‘commonly’ followed procedure is not free from drawbacks and requires leaps of faith. Underlying premises are: (1) the quartz luminescence signals are stable over time, (2) their test dose response corrections are accurate, (3) those quartz samples have a suitable “average behaviour” (compared to other natural quartz) and (4) they are highly representative. Furthermore, Hansen et al. (2015, 2018) have shown that, for reasons not yet fully understood, the variability of the calibration dose rates obtained using different batches of the RCQ, or within one batch for different periods of measurement, is

### 1. Introduction

The calibration of any artificial  $\beta$ -source commonly attached to a luminescence reader is a fundamental step for applying luminescence dating methods. However, despite its importance for the overall accuracy and comparability of the results obtained across luminescence dating laboratories worldwide, no calibration procedure largely validated and performed by the luminescence community has been agreed on during the last 30 years. As a consequence, each luminescence dating laboratory defines its calibration strategy, although a few studies have drawn attention to difficulties encountered with different materials and to sample specific effects (e.g., optical attenuation), with the measurement procedures and with the physics of  $\beta$ -particles themselves, including build-up and backscattering effects as well as non-uniformity of the dose rate due to field gradients test (e.g., Aitken 1985 and references therein; Bell & Mejdahl 1981;

much higher than expected: “any calibration can be up to 10% (95% probability) away from the mean” (Hansen et al., 2015).

At the IRAMAT-CRP2A luminescence dating laboratory in Bordeaux, the two commercially available ‘calibration quartz’ samples are routinely measured for estimating  $\beta$ -sources dose rates by applying SAR OSL. We repeat these tests for each  $\beta$ -source attached to a luminescence reader at least twice a year to verify the dose rates. The average dose rate and the associated uncertainty for a given source are determined from the entire (growing) time series. Additionally, considering the potential limitations of these two materials, quartz originating from various dating studies have also been investigated recently.

In practice, whereas Hansen et al. (2015, 2018) focused on multi-grain measurements and compared different batches of the same quartz or, different quartz (or feldspars) irradiated with the same facility, here we report single grain measurements for all the quartz samples considered here: RCQ, LCQ and quartz samples of different origins that were  $\gamma$ -irradiated with different facilities.

Our contribution does not aim at discarding or favouring a specific calibration material or  $\gamma$ -source but aims at encouraging discussions on this important topic which we believe to be of relevance for the upcoming Trapped Charge Dating Association.

## 2. Material and Methods

Table 1 summarises the different quartz samples that were used as calibration materials, and which are grouped into three categories according to their provenance. Table 2 summarises central information available in the literature for the employed  $\gamma$ -source facilities and the method used for their calibration. At Munich and Risø, the air kerma is deduced from measurements with an ionisation chamber, calibrated against a primary beam. The air kerma for such a beam is generally known with a high precision ( $< 0.5\%$ ) and the facilities follow ISO standards (for Munich, e.g., Greiter et al. 2016). However, the geometry of the quartz grain container differs as well as the mode of calculation of the dose to quartz (analytic against numeric – Monte Carlo Markov Chain). The  $\gamma$ -facility at the “*Laboratoire des Sciences du Climat et de l'Environnement*” (LSCE, Gif-sur-Yvette, France) is not directly calibrated with an ionization chamber, but calibration results from comparisons of TL signals (for quartzite pebbles) for this beam and a secondary  $^{60}\text{Co}$  beam (Table 2).

**Group (A).** It includes five batches of RCQ (see Hansen et al. 2015, 2018 for details about origin, preparation and characteristics): #40, #90, #106 and #113, plus one batch that was provided in 2013 but was not tagged with a specific batch number; henceforth it will be called “#2013”. For four out of the five batches, the granulometric fraction of

Table 1. List of samples with the corresponding SAR parameters. Each dose-response curve was fitted with a single saturating exponential. The stimulation time was 1 s, and the first 0.06 s and last 0.12 s were taken for signal and background respectively.

sample	supplier	geological / archaeological origin	grain size	preheat/cut/heat	optical wash	regenerative doses (s) / test doses (s)
RCQ #40	DTU Nutech	sand dune, Rømø, Jutland, South western Denmark (Tindahl Madsen et al., 2007; Hansen et al., 2015)	~120 $\mu\text{m}$	260 °C 10 s / 220 °C 10 s	280 °C 40 s	20,35,45,90,0,20/20
RCQ #90	DTU Nutech		180–225 $\mu\text{m}$	260 °C 10 s / 220 °C 10 s	280 °C 40 s	20,35,45,90,0,20/20
RCQ #106	DTU Nutech		180–225 $\mu\text{m}$	260 °C 10 s / 220 °C 10 s	280 °C 40 s	20,35,45,90,0,20/20
RCQ #113	DTU Nutech		180–225 $\mu\text{m}$	260 °C 10 s / 220 °C 10 s	280 °C 40 s	20,35,45,90,0,20/20
RCQ #2013	DTU Nutech		180–225 $\mu\text{m}$	260 °C 10 s / 220 °C 10 s	280 °C 40 s	20,35,45,90,0,20/20
LCQ	Freiberg Instruments GmbH	sand dune, Schletau, Germany (Hilgers 2007; Breest et al. 2001; Tolksdorf et al. 2013; Turner et al. 2013; D. Richter, pers. comm.)	~120 $\mu\text{m}$	200 °C 10 s / 200 °C cut	no	10,20,30,60,0,20/20
SB7	IRAMAT-CRP2A	Sibudu Cave, South Africa	200–250 $\mu\text{m}$	260 °C 10 s / 240 °C cut	280 °C 40 s	700,1400,2800,5600,0,700/250
SB12	IRAMAT-CRP2A	Sibudu Cave, South Africa	200–250 $\mu\text{m}$	260 °C 10 s / 240 °C cut	280 °C 40 s	300,600,1200,2400,4800,0,300/250
DRS5	IRAMAT-CRP2A	Diepkloof Rock Shelter, South Africa	200–250 $\mu\text{m}$	260 °C 10 s / 160 °C cut	no	400,800,1600,3200,0,400/400
DRS9	IRAMAT-CRP2A	Diepkloof Rock Shelter, South Africa	200–250 $\mu\text{m}$	260 °C 10 s / 220 °C 10 s	no	400,800,1600,3200,0,400/400
DRS11	IRAMAT-CRP2A	Diepkloof Rock Shelter, South Africa	200–250 $\mu\text{m}$	260 °C 10 s / 220 °C 10 s	no	600,1200,2400,4800,0,600/400
BRS2	IRAMAT-CRP2A	Bushman Rock Shelter, South Africa	200–250 $\mu\text{m}$	260 °C 10 s / 160 °C cut	no	100,200,400,800,0,100/100
UBB5	IRAMAT-CRP2A	Umbeli Belli, South Africa	200–250 $\mu\text{m}$	260 °C 10 s / 220 °C 10 s	no	400,800,1600,3200,0,400/400
UBB6	IRAMAT-CRP2A	Umbeli Belli, South Africa	200–250 $\mu\text{m}$	260 °C 10 s / 220 °C 10 s	no	400,800,1600,3200,0,400/400

Table 2. Main characteristics for the  $\gamma$ -irradiation facilities employed in this study and procedure for estimating the given dose.

facility	radioisotope	calibration of the $\gamma$ -source	dosing of the "calibration" quartz			reference
			packing	geometry of irradiation	calculation of the $\gamma$ -dose to quartz	
Risø	$^{137}\text{Cs}$	Ionisation chamber measuring air kerma, calibrated at the National Physical Laboratory, United Kingdom. Air kerma known at $\pm 1\%$	5 g of loose grains in a planar 100 x 100 x 4.8 mm <sup>3</sup> glass cell (2 mm wall thickness, 1 mm cavity; inner volume 6.5 cm <sup>3</sup> ) wrapped in black plastic	Irradiation in a beam at a distance of 2 m in a calibrated scatter-free geometry using a point-source of $^{137}\text{Cs}$	Calculation of the $\text{SiO}_2$ kerma considering the mass-energy absorption coefficients for $\text{SiO}_2$ and air; calculation of the $\gamma$ -attenuation in the cell and quartz grains volume assuming charge particle equilibrium and exponential attenuation law. Dose absorbed by $\text{SiO}_2$ = calibrated air kerma x ( $\text{SiO}_2$ kerma/air kerma) x attenuation	Hansen et al. (2015); Bos et al. (2006); A. Murray., pers. comm.
Munich	$^{137}\text{Cs}$	Ionization chamber, calibrated against the primary standard of the PTB, Germany. Air kerma known at $\pm 1\%$	Loose grains in a planar 45 x 12.5 x 12.5 mm <sup>3</sup> glass cell (wall thickness 4.2 and 4.3 mm, 5 mm cavity; inner volume 1.75 cm <sup>3</sup> )	Irradiation in a beam at a distance of 1 m from the $^{137}\text{Cs}$ source; the field radiation is not exactly parallel at this location and an additional 1.2% uncertainty is taken into account.	Absorbed dose in quartz per air kerma calculated using the Monte Carlo Code MCNPX 5 (X-5 Monte Carlo Team, 2003). Estimated error of the Monte Carlo approach: 1.4%. The total error on the dose (2.1%) combines (quadratically) with this uncertainty, the uncertainty of the air kerma and the uncertainty due to the geometry of the field.	D. Richter (pers. comm.); Greiter et al. (2016)
LSCE	$^{137}\text{Cs}$	Comparing TL signals (for 12 different crushed quartzite pebbles) after irradiation with a $^{60}\text{Co}$ beam (secondary French National beam) for one set of aliquots and with the LSCE $\gamma$ -source for another set of aliquots.	60 mg of loose grains in cylindric plastic cells (height: 6 mm)	Six sources of $^{137}\text{Cs}$ are located along a circular ring (diameter 5 cm). The cell containing the grains is located at the center where the vertical flux of $\gamma$ -rays is homogeneous (< 0.5% variability).	The calibration dose rate of this $\gamma$ -source is known by comparison of the TL signals of crushed quartzite pebbles obtained after irradiation in a primary source (see column 3).	Valladas (1978); Mercier et al. (2012)

the quartz grains is 180–250  $\mu\text{m}$ , but it is much smaller (about 120  $\mu\text{m}$ ) for batch #40. For batch #106, both the unirradiated and  $\gamma$ -irradiated ( $4.81 \pm 0.14$  Gy) fractions were available whereas batches #40, #113, and #2013 were limited to the irradiated fraction ( $4.81 \pm 0.14$  Gy). For #90, only the 0 Gy (zero dose) fraction was usable, since the 4.81 Gy fraction had been exhausted for calibrating other equipment. This fraction received a dose of 5 Gy ( $\pm 3\%$ ) using the  $\gamma$ -source facility of the LSCE (Valladas, 1978).

**Group (B).** This group consists of the first batch of the LCQ provided by Freiberg Instruments GmbH (D. Richter, pers. comm.). Two subsamples are available: one had been irradiated ( $3.00 \pm 0.06$  Gy) with a  $^{137}\text{Cs}$   $\gamma$ -source “Buchler Gammakalibrator OB 20” at the IAEA/WHO Secondary Standard Dosimetry Laboratory (SSDL) of the Helmholtz Zentrum München (D. Richter, pers. comm.); facility: Greiter et al. 2016) (henceforth termed ‘Munich’) and a second subsample, not dosed, was also provided.

**Group (C).** This group combines eight different quartz samples originating from four South African prehistoric sites: Sibudu (SB7 and SB12), Bushman Rock Shelter (BRS2), Umbeli Belli (UBB5 and UBB6), and Diepkloof Rock Shelter (DRS5, DRS9 and DRS11) (e.g., Tribolo et al., 2013; Soriano et al., 2015; Porraz et al., 2018; Bader et al., 2018). All these samples have been naturally bleached during the Middle Stone Age period and have then received potentially measurable equivalent doses. Except for Sibudu and Umbeli Belli, which are distant from each other only by few tens of kilometres, the sites are separated by more than 1,000 km. We therefore consider those quartz samples as being of different origins. They are all bright and their OSL signal is dominated by a fast component (checked with LM-OSL (Bulur, 1996) measurements and compared to the RCQ). For all of them, the 200–250  $\mu\text{m}$  granulometric fraction was available. The quartz samples were bleached twice for one minute in a Hönle SOL500 solar simulator with, at least, a pause of three hours between the two bleaching steps. Each bleached sample was divided into two subgroups: one was kept unirradiated and the other part was sent to the LSCE for  $\gamma$ -irradiation. For calibrating our  $\beta$ -source, we administered large doses between 30 Gy and 180 Gy ( $\pm 3\%$ ), which were chosen to be similar in size to natural doses.

All quartz samples were mounted on single grain (SG) discs facilitating 100 holes (theoretical diameter: 300  $\mu\text{m}$ ; depth: 300  $\mu\text{m}$ ). All these discs are supposed to be identical; however, they differ for several reasons: (1) SG discs tend to become worn out over time, i.e. the coating degrades and eventually falls apart. (2) Different batches of discs bought at different times do not have precisely the same characteristics, e.g., the diameters and depth of the holes are larger for some batches (closer to 350  $\mu\text{m}$ ) than for the other batches. To test the influence of the disc condition and geometry on the apparent calibration dose rate we measured

one material (RCQ, #113) with different sets of discs: new, old with small holes, and almost new with large holes.

All measurements were performed on a single machine (and with a single carousel): a Risø TL-OSL DA-20 single grain reader (basic design: Bøtter-Jensen et al. 2000). A 10 mW Nd:YVO<sub>4</sub> diode-pumped green laser (532 nm) was used for stimulation and the luminescence signal was detected with a PDM9107-CP-TTL photomultiplier tube through a combination of Hoya U340 glass filters (3 x 2.5 mm). The  $\beta$ -source  $^{90}\text{Sr}/^{90}\text{Y}$  attached to this reader has a nominal activity of 1.2 GBq. The irradiation field of this source revealed a non-uniformity that needs to be corrected and taken into account for the data analysis. To perform the correction, we used the software ‘CorrSGbin’ provided by DTU Nutech (Lapp et al., 2012). However, in our experiments, we found that the mean dose rate appeared to be unaffected by this correction (data not shown).

Before starting the calibration measurements, the efficiency of the SAR protocol was systematically checked: a  $\beta$ -dose was given by the source attached to the reader to the unirradiated fractions (i.e. RCQ #106, LCQ, all the South African quartz). When no unirradiated fraction was available (for the RCQ batches #40, #113 and #2013), the zero dose quartz of RCQ#106 was analysed, assuming that all the RCQ batches would support the same protocol on the same machine; a behaviour confirmed by our time series calibrations. For each measured aliquot, the normalized ( $L_x/T_x$ ) OSL signals were fitted with a saturating exponential:  $L_x/T_x = a * (1 - \exp^{-(b+D)/D_0})$ , where  $D$  is the regenerative dose and  $a$ ,  $b$  and  $D_0$  are fitting parameters. Table 1 summarises the parameters (preheat temperatures) and measurements conditions (regenerative doses) applied for each sample.

A series of rejection criteria were used for the grain selection: (1) natural test dose signal at least 3 times above background, (2) natural test dose relative error  $< 10\%$ , and (3) recuperation  $< 5\%$  of the natural signal. Note that, according to our own observations, the recycling ratio seems not to be a key criterion as already suggested by, e.g., Guérin et al. (2015) and Thomsen et al. (2016), and was thus not used as a selection criterion. In addition, since for some of our quartz samples the given dose is high (up to 180 Gy) and may, therefore, induce signal saturation problems for some of the grains, an additional criterion was applied based on the saturation parameter  $D_0$  (cf. Thomsen et al., 2016).

For each series of measurements, the central dose model (Galbraith et al., 1999) was applied for calculating the final dose and hence, the apparent dose rate of our  $\beta$ -source.

The software *Analyst* (v4.52; Duller 2015) was used for the data analyses. Plots were produced using the **R** (R Core Team, 2018) package ‘Luminescence’ (Kreutzer et al., 2012, 2018).

Table 3. Dose recovery ratio and calibration dose rates obtained for the different samples. We used the adjectives “old” to describe SG discs that were somewhat worn out, “new” to label so far untouched discs and “large” to label discs with holes that are larger than they are for the “new” and “old disc” (see main text). The  $\gamma$ -doses have associated relative uncertainties at one sigma of 3% for the LSCE and Risø facilities and 2% for the Munich facility. Where indicated, the dose recovery tests were performed with the unirradiated part of the sample just before the calibration measurements. The  $\times$  symbol indicates that the test was performed just before the calibration measurement, but on the 0 Gy RCQ fraction of #106. The calibrations were performed over several months but for comparison, all the dose rates are re-calculated for 2018-10-25. n/N indicates the number of accepted over the number of measured grains (1) for the dose recovery tests, (2) for the calibration measurements. The sensitivity change is based on the “test-signal-change” calculated in Analyst, corresponding to the ratio between the last and first test dose signal.

sample	disc	given γ-dose (Gy)	γ- source	date of measure- ment	dose recovery tests			dose rate measurements				
					n/N <sup>(1)</sup>	dose recovery ratio	OD (%)	sensitivity change	n/N <sup>(2)</sup>	calculated dose rate on 2018-10-25	OD (%)	sensitivity change
RCQ#106	old	4.81	Risø	Jan-17	265/400	1.06 ± 0.01	9 ± 1	0.8 ± 0.2	254/400	0.106 ± 0.002	12 ± 1	0.9 ± 0.2
RCQ#106	old	4.81	Risø	Jul-17	257/400	1.00 ± 0.01	5 ± 1	0.8 ± 0.2	319/400	0.105 ± 0.002	17 ± 1	0.9 ± 0.2
RCQ#106	old	4.81	Risø	Sep-17	298/400	1.11 ± 0.01	22 ± 1	0.8 ± 0.2	339/400	0.104 ± 0.002	12 ± 1	0.9 ± 0.2
RCQ#2013	new	4.81	Risø	May-18	256/400	×1.02 ± 0.01	7 ± 1	0.8 ± 0.2	202/800	0.123 ± 0.002	13 ± 1	4.1 ± 3.2
DRS9	old	100	LSCE	May-18		nd			71/1700	0.127 ± 0.002	10 ± 2	1.1 ± 0.3
RCQ#113	new	4.81	Risø	May-18	271/400	×1.00 ± 0.00	0	0.8 ± 0.2	255/400	0.104 ± 0.002	19 ± 1	1.1 ± 0.3
RCQ#113	old	4.81	Risø	May-18		nd			279/400	0.108 ± 0.002	10 ± 1	1.2 ± 0.3
RCQ#113	new	4.81	Risø	May-18		nd			256/400	0.106 ± 0.002	10 ± 1	1.1 ± 0.3
RCQ#113	large	4.81	Risø	May-18		nd			289/400	0.104 ± 0.002	0	1.1 ± 0.2
LCQ	old	3	Munich	May-18		nd			65/300	0.127 ± 0.004	11 ± 2	0.7 ± 0.2
DRS9	old	100	LSCE	May-18	70/800	1.03 ± 0.02	12 ± 2	1.1 ± 0.3	64/1100	0.126 ± 0.003	10 ± 2	1.1 ± 0.3
DRS11	old	100	LSCE	May-18	26/800	0.96 ± 0.01	16 ± 2	1.2 ± 0.3	26/500	0.117 ± 0.003	9 ± 2	1.2 ± 0.3
DRS5	old	100	LSCE	Jun-18	47/700	1.01 ± 0.02	9 ± 2	1.4 ± 0.5	27/700	0.111 ± 0.005	18 ± 4	1.5 ± 0.5
RCQ#90	old	5	LSCE	Sep-18		nd			316/400	0.122 ± 0.001	10 ± 1	1.0 ± 0.2
RCQ#113	old	4.81	Risø	Sep-18		nd			262/400	0.111 ± 0.001	9 ± 1	1.2 ± 0.3
BR52	old	30	LSCE	Sep-18	201/300	1.03 ± 0.01	10 ± 1	1.1 ± 0.3	335/500	0.120 ± 0.004	11 ± 1	1.2 ± 0.4
SB12	old	80	LSCE	Sep-18	85/300	1.03 ± 0.02	15 ± 2	1.0 ± 0.34	83/300	0.124 ± 0.003	15 ± 2	0.9 ± 0.3
UBB5	old	45	LSCE	Sep-18	143/500	0.95 ± 0.01	12 ± 0	1.3 ± 0.4	165/500	0.126 ± 0.004	14 ± 1	1.3 ± 0.4
UBB6	old	100	LSCE	Sep-18	58/700	1.00 ± 0.02	12 ± 3	1.0 ± 0.2	43/700	0.124 ± 0.005	14 ± 3	1.0 ± 0.2
SB7	old	180	LSCE	Oct-18	24/600	1.03 ± 0.04	12 ± 3	0.8 ± 0.2	50/600	0.114 ± 0.005	16 ± 2	0.8 ± 0.2
RCQ#113	old	4.81	Risø	Sep-18	227/400	×1.00 ± 0.01	2 ± 1	0.8 ± 0.2	262/400	0.109 ± 0.001	10 ± 1	1.2 ± 0.4
RCQ#2013	old	4.81	Risø	Sep-18		nd			99/400	0.117 ± 0.002	12 ± 1	3.3 ± 1.6
RCQ#40	old	4.81	Risø	Sep-18		nd			30/400	0.111 ± 0.003	10 ± 2	0.7 ± 0.2
LCQ	old	3	Munich	Oct-18	108/600	1.00 ± 0.01	7 ± 2	0.8 ± 0.2	98/600	0.125 ± 0.003	15 ± 2	0.8 ± 0.2



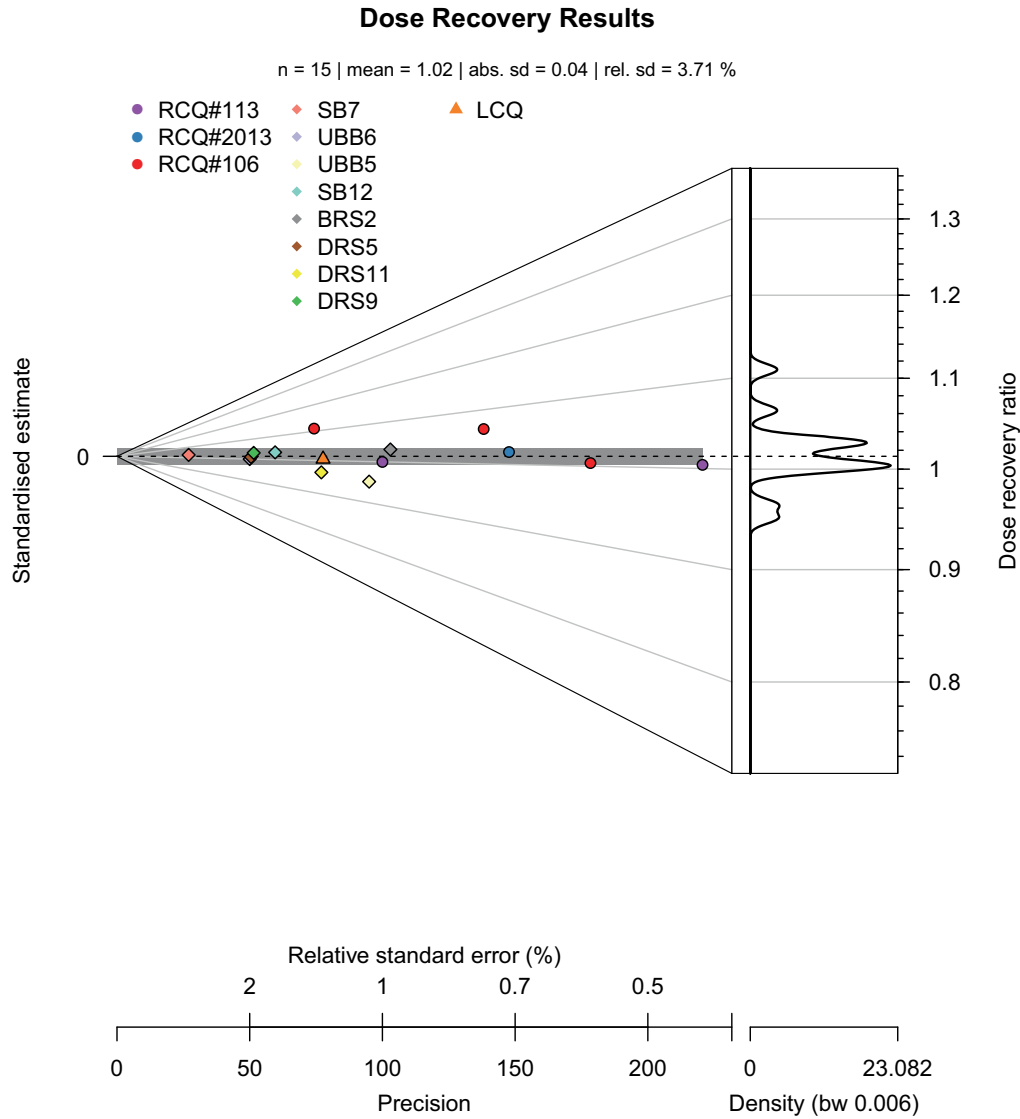


Figure 1. Abanico plot (Dietze et al., 2016) of the dose recovery ratio. Different samples are colour coded. Circles display samples irradiated at Risø; rectangle show samples irradiated at the LSCE; triangles are used for samples irradiated at Munich.

### 3. Results

Results are presented in Table 3 and in Figures 1 and 2. Except for one case (RCQ#106 from September 2017), the dose recovery ratios are consistent with unity or within 5% of unity. The central<sup>1</sup> ratio for all the data is  $1.02 \pm 0.01$  with an overdispersion (OD) of  $3 \pm 1\%$  (Fig. 1).

The apparent dose rates deduced from the calibration measurements show a significant dispersion ( $0.115 \pm 0.002$  Gy/s, OD  $7 \pm 1\%$ ). Two dose rate groups can be distinguished: the first includes the LCQ (irradiated in Munich), all the South African quartz samples and the RCQ #90 irradiated at the LSCE, as well as the RCQ #2013

(irradiated at DTU Nutech) (central dose:  $0.122 \pm 0.001$  Gy/s, OD:  $2 \pm 1\%$ ). The second group includes the RCQ #113, #40 and #106 and potentially, two south African quartz samples having a lower precision (SB7 and DRS5) (central dose:  $0.107 \pm 0.001$  Gy/s, OD:  $2 \pm 1\%$ ). The 14% difference between the central dose values for these two groups is statistically significant (two-sided paired *t*-test, *p*-value:  $< 0.01$ ).

Note 1: Additionally, we have performed a few multiple grain measurements on other readers with similar results. To keep the text concise, only the SG measurements for one reader are reported.

Note 2: The 12% discrepancy between one of the RCQ (#2013) alone and the other RCQ (#40, #106, #113) is consistent with those reported by Hansen et al. (2015, 2018).

<sup>1</sup>In all the data presented here, the differences between the arithmetic mean and the central dose rates following Galbraith et al. (1999) are negligible.

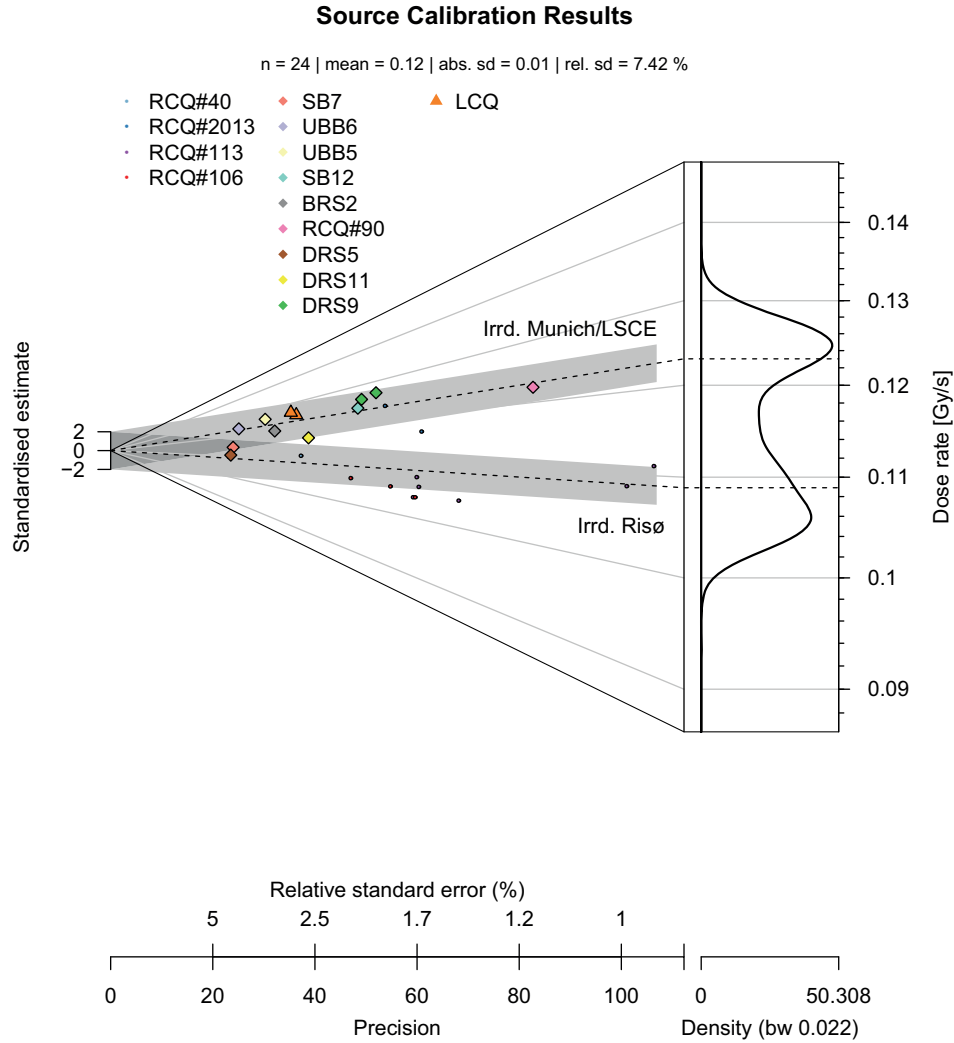


Figure 2. Abanico plot (Dietze et al., 2016) of the obtained calibration dose rates. Different samples are colour coded (similar to Fig. 1). Circles display samples irradiated at Risø; rectangles show samples irradiated at the LSCE; triangles are used for samples irradiated at Munich.

#### 4. Discussion

The mean sensitivity changes vary for all samples except for RCQ#2013, between  $0.7 \pm 0.2$  and  $1.5 \pm 0.5$  (ratio of last and first test dose signal; Table 3). As expected, they are similar for the non-irradiated and the corresponding  $\gamma$ -irradiated samples. This is unfortunately not true for RCQ#2013 whose mean sensitivity changes are significantly higher ( $4.1 \pm 3.2$  and  $3.3 \pm 1.6$ ). This weakens the use as a surrogate for dose recovery test of RCQ#106 and might explain partly why this RCQ quartz gives an apparent dose rate significantly different from the other RCQ. Except for RCQ#2013, we did not observe correlations between the sensitivity changes and the apparent dose rates (data not shown).

The consistency of the dose recovery ratio with unity and the low OD observed there ( $3 \pm 1\%$ , compared to the  $2 \pm 1\%$  observed for each calibration group) suggests that neither

the protocol nor the stability of the equipment is responsible for the observed differences between the calibration dose rates. The  $2 \pm 1\%$  OD for each group may reflect small “behavioural” differences between the quartz samples.

The software *CorrSGbin* (Lapp et al., 2012) was applied to the data before the analyses to correct for the non-uniformity of the  $\beta$ -radiation field of the source. Besides, the grains that are selected for the apparent dose rate calculations are sufficiently numerous and well spread over the discs, so that any remaining effect of non-uniformity unlikely caused the observed discrepancy. Figure 3 illustrates our assumption for two examples: RCQ#113 irradiated with the Risø  $\gamma$ -source, and RCQ#90 irradiated in LSCE. All the positions are covered and for a large majority of them, the apparent dose rates of the RCQ#90 are larger than the apparent dose rates of the RCQ#113.

For the first group of calibration dose rates, the consis-



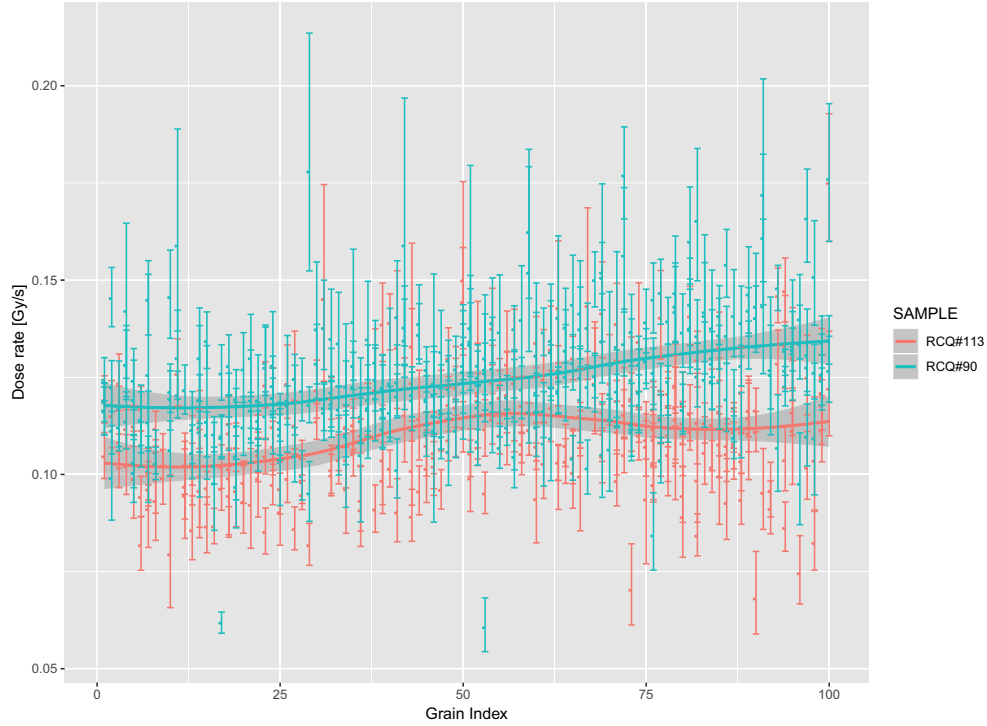


Figure 3. Plot of the apparent dose rate as a function of the grain position on the disc (numbered from 1 to 100). Red dots: RCQ#113, irradiated 4.81 Gy at Risø; turquoise dots: RCQ#90 irradiated with 5 Gy at Gif-sur-Yvette. Error bars represent the individual standard error of each value. While the dose rates between the two batches differ significantly, the variation between the grain positions appears to be random, with a very small increase towards grain position 100.

tency of the results suggests that neither the provenance of the quartz (see also Hansen et al. 2018) nor the value of the artificially given dose (and potential saturation problems)

is responsible for the observed discrepancy. For the second group of calibration dose rates which includes #40 (smaller diameter of quartz grains, implying more than one grain per hole) and all the measurements made with different type-s/qualities of SG discs (#113), we deduce that neither the grain size (ca. 100  $\mu\text{m}$  vs ca. 200  $\mu\text{m}$ ), nor the condition of the SG discs is responsible for the observed variability.

Consequently, according to our measurements and observations, it seems that the primary source for the discrepancy between the two groups of apparent dose rates is the  $\gamma$ -dose delivered by the three irradiation facilities.

For most dating applications, a discrepancy of 14% between two estimates of calibration dose rates is hardly acceptable since a similar offset would be observed in resulting luminescence ages and such value is larger than the average age uncertainties of ca. 9% usually reported ( $Q_{0.25}$ : 6.8%,  $Q_{0.75}$ : 12.7%,  $n_{\text{valid}} = 3,484$ ; source: INQUA Dune Atlas, Lancaster et al. 2015). Nonetheless, based on the results presented here, it appears that the current systematic uncertainty of 2% to 4% for the calibration dose rate usually reported might be underestimated.

Since the standard error (SE) of the source calibration impacts all individual doses similarly measured with one reader, it may be considered as a systematic error (cf. Aitken, 1985). To obtain the final standard error for a luminescence age, the following equation can be used:

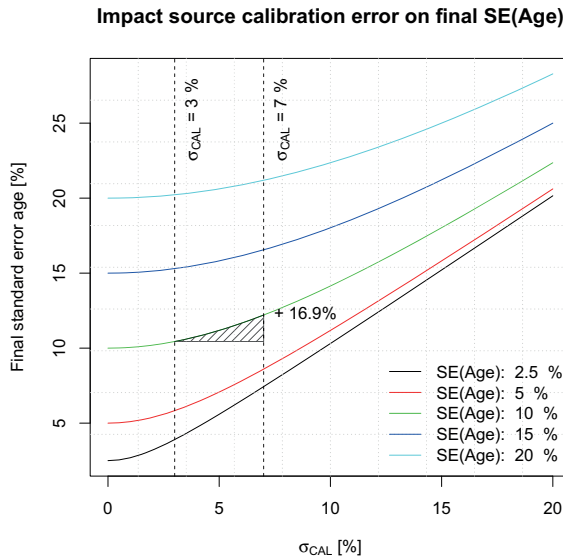


Figure 4. Isoline plots showing the impact of the uncertainty on the calibration dose rate on the final standard error on the age, for various values of  $\sqrt{\left(\frac{\sigma_D}{D}\right)^2 + \left(\frac{\sigma_{D_e}}{D_e}\right)^2}$

$$\left(\frac{\sigma_A}{A}\right)^2 = \left(\frac{\sigma_D}{D}\right)^2 + \left(\frac{\sigma_{D_e}}{D_e}\right)^2 + \left(\frac{\sigma_{D_{CAL}}}{D_{CAL}}\right)^2$$

where  $\sigma_A$  is the total absolute uncertainty of the age  $A$ ,  $\sigma_D^2$  is the quadratic sum of the absolute systematic and statistical uncertainties of the environmental dose rate  $\dot{D}$ ,  $\sigma_{D_e}^2$  is the quadratic absolute uncertainty of the equivalent dose  $D_e$ , and  $\sigma_{D_{CAL}}^2$  is the quadratic systematic absolute uncertainty on the calibration dose rate  $D_{cal}$ . Figure 4 displays plots of  $\frac{\sigma_A}{A}$  as function of  $\frac{\sigma_{D_{CAL}}}{D_{CAL}}$  for various values of  $\sqrt{\left(\frac{\sigma_D}{D}\right)^2 + \left(\frac{\sigma_{D_e}}{D_e}\right)^2}$  (termed SE(Age) in Fig. 4), from 2.5% to 20%. For example, if this quantity is 10% and the relative uncertainty of the calibration dose rate,  $\frac{\sigma_{D_{CAL}}}{D_{cal}}$ , is 7% instead of 3%, it would imply an increase of the coefficient of variation on the age of ca. 17%, from 10.4% to 12.2%. Whether this is acceptable or not depends on the chronological context. Nonetheless, contrary to the various factors used in the age equation for which the uncertainty is both difficult to evaluate precisely, and/or difficult to reduce (water contents, dosimetric heterogeneity, long-term luminescence signal behaviour issues etc.), it seems that the uncertainty of the calibration dose rate could be improved and properly handled.

## 5. Conclusion

By using a series of different quartz samples ('calibration' quartz commercially available and quartz samples prepared at the IRAMAT-CRP2A), we performed SAR OSL measurements that aimed at determining apparent dose rates for one of our in-built  $\beta$ -source. High variability was observed, and our experiments lead us to conclude that the doses delivered by different irradiation facilities might not be comparable (two groups with a different apparent dose rate of ca. 14%). As a consequence, our observations, in conjunction with those already reported by Hansen et al. (2015, 2018), suggest that the systematic error of 2% to 4% for the calibration dose rate usually reported by the luminescence dating community in dating studies might be underestimated. The source of the observed discrepancy needs to be further investigated. At the IRAMAT-CRP2A, we will continue our investigations with samples irradiated by more than the three here already compared  $\gamma$ -irradiators.

## Acknowledgments

The work was supported by the LaScArBx. LaScArBx is a research programme supported by the ANR (ANR-10-LABX-52). It was also funded by the Conseil Régional Nouvelle Aquitaine (project DAPRES\_LA\_FEM) and the ANR (project DOM-ART n° ANR-16-CE27-0004-01). We are grateful to Hélène Valladas who performed the  $\gamma$ -irradiation at the LSCE. Thanks to Daniel Richter for sharing information on the LexCal quartz and for discussions. David Sander-son provided a very constructive review.

## References

- Aitken, M. J. *Thermoluminescence dating*. Studies in archaeological science. Academic Press, 1985.
- Bader, G. D., Tribolo, C., and Conard, N. J. *A return to Umbel Belli: New insights of recent excavations and implications for the final MSA of eastern South Africa*. Journal of Archaeological Science: Reports, 21: 733–757, 2018. doi: 10.1016/j.jasrep.2018.08.043.
- Bell, W. T. and Mejdahl, V. *Beta Source Calibration and Its Dependency on Grain Transparency*. Archaeometry, 23(2): 231–240, 1981. doi: 10.1111/j.1475-4754.1981.tb00310.x.
- Bos, A. J. J., Wallinga, J., Johns, C., Abellon, R. D., Brouwer, J. C., Schaart, D. R., and Murray, A. S. *Accurate calibration of a laboratory beta particle dose rate for dating purposes*. Radiation Measurements, 41(7-8): 1020–1025, 2006. doi: 10.1016/j.radmeas.2006.04.003.
- Bøtter-Jensen, L., Bulur, E., Duller, G. A. T., and Murray, A. S. *Advances in luminescence instrument systems*. Radiation Measurements, 32(5-6): 523–528, 2000. doi: 10.1016/S1350-4487(00)00039-1.
- Breest, K., Veil, S., Heinemann, B., Hilgers, A., and Willerding, U. *Die Ausgrabungen auf dem mesolithischen Dünenfundplatz Schletau 2000, Ldkr. Lüchow-Dannenberg*. Die Kunde N F, 52: 239–254, 2001.
- Bulur, E. *An Alternative Technique For Optically Stimulated Luminescence (OSL) Experiment*. Radiation Measurements, 26(5): 701–709, 1996. doi: 10.1016/S1350-4487(97)82884-3.
- Dietze, M., Kreutzer, S., Burow, C., Fuchs, M. C., Fischer, M., and Schmidt, C. *The abanico plot: visualising chronometric data with individual standard errors*. Quaternary Geochronology, 31: 12–18, 2016. doi: 10.1016/j.quageo.2015.09.003.
- Duller, G. A. T. *The Analyst software package for luminescence data: overview and recent improvements*. Ancient TL, 33 (1): 35–42, 2015. URL [http://ancienttl.org/ATL\\_33-1\\_2015/ATL\\_33-1\\_Duller\\_p35-42.pdf](http://ancienttl.org/ATL_33-1_2015/ATL_33-1_Duller_p35-42.pdf).
- Erfurt, G., Krbetschek, M. R., Trautmann, T., and Stolz, W. *Radioluminescence (RL) probe dosimetry using Al<sub>2</sub>O<sub>3</sub>:C for precise calibration of beta sources applied to luminescence dating*. Radiation Physics and Chemistry, 61(3–6): 721–722, 2001. doi: 10.1016/S0969-806X(01)00386-3.
- Galbraith, R. F., Roberts, R. G., Laslett, G. M., Yoshida, H., and Olley, J. M. *Optical dating of single and multiple grains of Quartz from Jinmium Rock Shelter, Northern Australia: Part I, Experimental design and statistical models*. Archaeometry, 41(2): 339–364, 1999. doi: 10.1111/j.1475-4754.1999.tb00987.x.
- Göksu, H. Y., Bailiff, I. K., Bøtter-Jensen, L., Brodski, L., Hütt, G., and Stoneham, D. *Interlaboratory beta source calibration using TL and OSL on natural quartz*. Radiation Measurements, 24(4): 479–483, 1995.
- Greiter, M. B., Denk, J., and Hoedlmoser, H. *Secondary Standard Calibration, Measurement and Irradiation Capabilities of the Individual Monitoring Service at the Helmholtz Zentrum München: Aspects of Uncertainty and Automation*. Radiation Protection Dosimetry, 170(1-4): 103–107, 2016. doi: 10.1093/rpd/ncv537.

- Guérin, G. and Valladas, H. *Cross-calibration between beta and gamma sources using quartz OSL: Consequences of the use of the SAR protocol in optical dating*. Radiation Measurements, 68 (c): 31–37, 2014. doi: 10.1016/j.radmeas.2014.06.010.
- Guérin, G., Frouin, M., Talamo, S., Aldeias, V., Bruxelles, L., Chiotti, L., Dibble, H. L., Goldberg, P., Hublin, J.-J., Jain, M., Lahaye, C., Madelaine, S., Maureille, B., McPherron, S. J. P., Mercier, N., Murray, A. S., Sandgathe, D., Steele, T. E., Thomsen, K. J., and Turq, A. *A multi-method luminescence dating of the Palaeolithic sequence of La Ferrassie based on new excavations adjacent to the La Ferrassie 1 and 2 skeletons*. Journal of Archaeological Science, 58(C): 147–166, 2015. doi: 10.1016/j.jas.2015.01.019.
- Hansen, V., Murray, A., Buylaert, J.-P., Yeo, E.-Y., and Thomsen, K. *A new irradiated quartz for beta source calibration*. Radiation Measurements, 81: 123–127, 2015. doi: 10.1016/j.radmeas.2015.02.017.
- Hansen, V., Murray, A., Thomsen, K., Jain, M., Autzen, M., and Buylaert, J.-P. *Towards the origins of over-dispersion in beta source calibration*. Radiation Measurements, pp. 1–6, 2018. doi: 10.1016/j.radmeas.2018.05.014.
- Hilgers, A. *The chronology of Late Glacial and Holocene dune development in the northern Central European lowland reconstructed by optically stimulated luminescence (OSL) dating*. PhD thesis, 2007.
- Kadereit, A. and Kreutzer, S. *Risø calibration quartz – a challenge for  $\beta$ -source calibration. An applied study with relevance for luminescence dating*. Measurement, 46(7): 2238–2250, 2013. doi: 10.1016/j.measurement.2013.03.005.
- Kreutzer, S., Dietze, M., Burow, C., Fuchs, M. C., Schmidt, C., Fischer, M., and Friedrich, J. *Luminescence: Comprehensive Luminescence Dating Data Analysis*. CRAN, version 0.8.6, 2018. URL <https://CRAN.R-project.org/package=Luminescence>.
- Kreutzer, S., Schmidt, C., Fuchs, M. C., Dietze, M., Fischer, M., and Fuchs, M. *Introducing an R package for luminescence dating analysis*. Ancient TL, 30(1): 1–8, 2012. URL [http://ancienttl.org/ATL\\_30-1\\_2012/ATL\\_30-1\\_Kreutzer\\_p1-8.pdf](http://ancienttl.org/ATL_30-1_2012/ATL_30-1_Kreutzer_p1-8.pdf).
- Lancaster, N., Wolfe, S., Thomas, D., Bristow, C., Bubenzer, O., Burrough, S., Duller, G., Halfen, A., Hesse, P., Roskin, J., Singhvi, A., Tsoar, H., Tripaldi, A., Yang, X., and Zárate, M. *The INQUA Dunes Atlas chronologic database*. Quaternary International, 410: 3–10, 2015. doi: 10.1016/j.quaint.2015.10.044.
- Lapp, T., Jain, M., Thomsen, K. J., Murray, A. S., and Buylaert, J. P. *New luminescence measurement facilities in retrospective dosimetry*. Radiation Measurements, 47: 803–808, 2012. doi: 10.1016/j.radmeas.2012.02.006.
- Mercier, N., Tribolo, C., Lahaye, C., and Hernandez, M. *Beta-source calibration with quartz: can we determine a single dose-rate?* In *Asia Pacific LED*, volume unpublished poster presentation, Japan, 2012.
- Murray, A. S. and Wintle, A. G. *Luminescence dating of quartz using an improved single-aliquot regenerative-dose protocol*. Radiation Measurements, 32(1): 57–73, 2000. doi: 10.1016/S1350-4487(99)00253-X.
- Pernicka, E. and Wagner, G. A. *Primary and interlaboratory calibration of beta sources using quartz as thermoluminescent phosphor*. Ancient TL, (6): 2–6, 1979.
- Porraz, G., Val, A., Tribolo, C., Mercier, N., de la Peña, P., Haaland, M. M., Igreja, M., Miller, C. E., and Schmid, V. C. *The MIS5 Pietersburg at ‘28’ Bushman Rock Shelter, Limpopo Province, South Africa*. PLOS ONE, 13(10): e0202853–45, 2018. doi: 10.1371/journal.pone.0202853.
- R Core Team. *R: A Language and Environment for Statistical Computing*. Vienna, Austria, 2018. URL <https://r-project.org>.
- Soriano, S., Villa, P., Delagnes, A., Degano, I., Pollarolo, L., Lucejko, J. J., Henshilwood, C., and Wadley, L. *The Still Bay and Howiesons Poort at Sibudu and Blombos: Understanding Middle Stone Age Technologies*. PLOS ONE, 10(7): e0131127–46, 2015. doi: 10.1371/journal.pone.0131127.
- Thomsen, K. J., Murray, A. S., Buylaert, J. P., Jain, M., Hansen, J. H., and Aubry, T. *Testing single-grain quartz OSL methods using sediment samples with independent age control from the Bordes-Fitte rockshelter (Roches d’Abilly site, Central France)*. Quaternary Geochronology, 31(C): 77–96, 2016. doi: 10.1016/j.quageo.2015.11.002.
- Tindahl Madsen, A., Murray, A. S., and Joest Andersen, T. *Optical Dating of Dune Ridges on Rømø, a Barrier Island in the Wadden Sea, Denmark*. Journal of Coastal Research, 23(5): 1259–12, 2007. doi: 10.2112/05-0471.1.
- Tolksdorf, J. F., Klasen, N., and Hilgers, A. *The existence of open areas during the Mesolithic: evidence from aeolian sediments in the Elbe-Jeetzel area, northern Germany*. Journal of Archaeological Science, 40(6): 2813–2823, 2013. doi: 10.1016/j.jas.2013.02.023.
- Tribolo, C., Mercier, N., Douville, E., Joron, J. L., Reyss, J. L., Rufer, D., Cantin, N., Lefrais, Y., Miller, C. E., Porraz, G., Parkington, J., Rigaud, J. P., and Texier, P. J. *OSL and TL dating of the Middle Stone Age sequence at Diepkloof Rock Shelter (South Africa): a clarification*. Journal of Archaeological Science, 40 (9): 3401–3411, 2013. doi: 10.1016/j.jas.2012.12.001.
- Turner, F., Tolksdorf, J. F., Viehberg, F., Schwalb, A., Kaiser, K., Bittmann, F., von Bramann, U., Pott, R., Staesche, U., Breest, K., and Veil, S. *Lateglacial/early Holocene fluvial reactions of the Jeetzel river (Elbe valley, northern Germany) to abrupt climatic and environmental changes*. Quaternary Science Reviews, 60: 91–109, 2013. doi: 10.1016/j.quascirev.2012.10.037.
- Valladas, G. *A gamma ray irradiator*. PACT 3 - Revue du Réseau Européen de Sciences et Techniques appliquées au Patrimoine Culturel, pp. 439–442, 1978.
- X-5 Monte Carlo Team. *MCNP — A General Monte Carlo N-Particle Transport Code, Version 5*. 2003. URL <https://laws.lanl.gov/vhosts/mcnp.lanl.gov/mcnp5.shtml>.

## Reviewer

David Sanderson